The effective density and fractal dimension of particles emitted from a light-duty diesel vehicle with a diesel oxidation catalyst

J.S. Olfert[a,*], J.P.R. Symonds[b], N. Collings[a]

[a] *Hopkinson Laboratory, Cambridge University Engineering Department, Trumpington Street, Cambridge CB2 1PZ, UK*
[b] *Cambustion Ltd., J6 The Paddocks, 347 Cherry Hinton Road, Cambridge CB1 8DH, UK*

Abstract

A differential mobility analyzer (DMA) and a Couette centrifugal particle mass analyzer (Couette CPMA) were used to measure the effective density and fractal dimension of particles emitted from a light-duty diesel vehicle fitted with a diesel oxidation catalyst (DOC). It was found that at high engine loads, the DOC increased in temperature, sulphate levels in the particulate matter increased, and a transient nucleation mode was observed. The increase in sulphate levels resulted in a drastic increase in the effective density and fractal dimension of the particles. At low engine loads (8–15%), sulphate levels were much lower, no nucleation mode was present and the fractal dimension varied from 2.22 to 2.48, which is in good agreement with previous studies. At 40% load, sulphate levels were much higher and the fractal dimension was 2.76.
© 2006 Elsevier Ltd. All rights reserved.

1. Introduction

Particles in the environment are known to affect climate change and reduce visibility. There is also evidence that suggests that particles can have a negative effect on human health. Particles can be generated by a variety of sources, both natural and anthropogenic; however, particulate emissions from diesel vehicles are a major source of ultra-fine particles in the atmosphere. Particles and aerosols can be characterized by many different properties such number concentration, mass concentration, particle size, mass, density, volume, dynamic shape factor, fractal dimension, etc. By measuring the mobility size and mass of particles, other important particle properties can be determined such as effective density and fractal dimension.

The particle effective density is an important parameter because it determines particle transport properties, it can be used to convert size distributions to mass distributions, and it provides a relationship between mobility and aerodynamics sizes. The morphology of an agglomerate is characterized by its fractal dimension. The morphology affects the behaviour

---

* Corresponding author. Brookhaven National Laboratory, Atmospheric Sciences Division, Building 815E, Upton, NY 11973-5000, USA. Tel.: +144 1223 332681; fax: +144 1223 339906.

E-mail addresses: j.s.olfert.03@cantab.net, jolfert@bnl.gov (J.S. Olfert).

of particles in the atmosphere (Friedlander, 2000) and possibly impacts upon the effect particles have on human health (Bérubé et al., 1999).

There have been several studies that have measured the effective density and/or fractal dimension of diesel exhaust particles. These studies have generally used a differential mobility analyzer (DMA) and an electrical low-pressure impactor (ELPI) to determine the particle's mobility and aerodynamic diameters, respectively. In general, two different experimental methods have been used to find the effective density and fractal dimension of diesel particles using a DMA and ELPI. The first method (used by Ahlvik et al., 1998; Maricq et al., 2000 to measure effective density, and Maricq and Xu, 2004 to measure effective density and fractal dimension) involves using a DMA and an ELPI in series, where particles are first classified by mobility size with the DMA and then the aerodynamic size is determined with the ELPI. The effective densities of diesel particles measured by Ahlvik et al. (1998) and Maricq et al. (2000) were much higher than later studies found. It was later suggested by Maricq and Xu (2004) that the effective densities were overestimated due to soot accumulation on the impactor plates. A similar technique was used by Skillas et al. (1998) and Van Gulijk et al. (2004) to measure the fractal dimension of diesel particles. A second technique, used by Virtanen et al. (2002), and Virtanen et al. (2004), involves using a scanning mobility particle sizer (SMPS) in parallel with an ELPI, where the difference between the two corresponding size distributions is minimized by fitting the data with a size-dependent effective density function (also see Virtanen et al., 2004 and Ristimäki et al., 2002 for a detailed description of this method). The effective density of diesel particles could also be determined by using other systems such as: a DMA, optical particle counter, and aerodynamic particle sizer (Hand and Kreidenweis, 2002), an SMPS and aerosol mass spectrometer (Katrib et al., 2004), and a DMA and a single particle laser ablation time-of-flight mass spectrometer (Zelenyuk et al., 2005). However, experiments using these other systems have not been conducted with diesel particles.

Park, Cao, Kittelson, and McMurry (2003) have shown that the effective density and fractal dimension of diesel particles can also be measured using a DMA and an aerosol particle mass analyzer (APM; Ehara et al., 1996) to measure particle mobility diameter and particle mass, respectively. Recently, a new particle mass classifier has been developed called the Couette centrifugal particle mass analyzer (Couette CPMA), which is similar to the APM, but with an improved transfer function (see Olfert and Collings, 2005 and Olfert et al., 2006). In this study, a DMA and Couette CPMA will be used to measure the effective density and fractal dimension of diesel particles produced from a light-duty diesel vehicle with a diesel oxidation catalyst (DOC).

Previous studies by Maricq et al. (2002); Vogt et al. (2003), and Giechaskiel et al. (2005) have shown that the size distribution of diesel soot can change with fuel sulphur levels and DOC temperature. However, previous studies have not shown how increased levels of sulphuric acid in the exhaust can drastically change the effective density and fractal dimension of diesel soot. The purpose of this study is to show how the Couette CPMA can be used to measure the effective density and fractal dimension of non-spherical particles (i.e. diesel particles), and show how increased levels of sulphate in the exhaust, due to increased DOC temperatures, can greatly increase the effective density and fractal dimension of diesel particles.

2. Experimental set-up

2.1. Sampling diesel exhaust

A schematic of the experimental set-up is seen in Fig. 1. The light-duty diesel vehicle used in this study was a 2002 Peugeot 406 (2.2 L common rail diesel) certified to Euro III standards. The vehicle was fitted with a DOC. The diesel fuel used had < 50 ppm of sulphur, although the exact concentration of sulphur was not measured, the same tank of fuel was used for all the tests. The vehicle was operated on a chassis dynamometer at six different engine speed/load settings. For each of the tests the vehicle was warmed-up by running the vehicle at the required setting for approximately 10 min before the test was started. Each test ran for approximately 1 h. The exhaust from the vehicle was diluted immediately (with air at 25 °C and 45% relative humidity) as it entered the constant volume sampling (CVS) dilution tunnel. The particles in the dilution tunnel were measured with three different systems. Firstly, a sample of the diesel soot was taken with filter paper (Pallflex Emfab filters; TX40HI20WW) for sulphate analysis. For each of the tests two sequential filter measurements were taken with each filter collecting samples for approximately 20 min. The sulphate was extracted from the filter and analysed with ion chromatography using a similar method as described by SAE J1936 (1989). Secondly, the size distribution was continuously measured with a differential mobility spectrometer
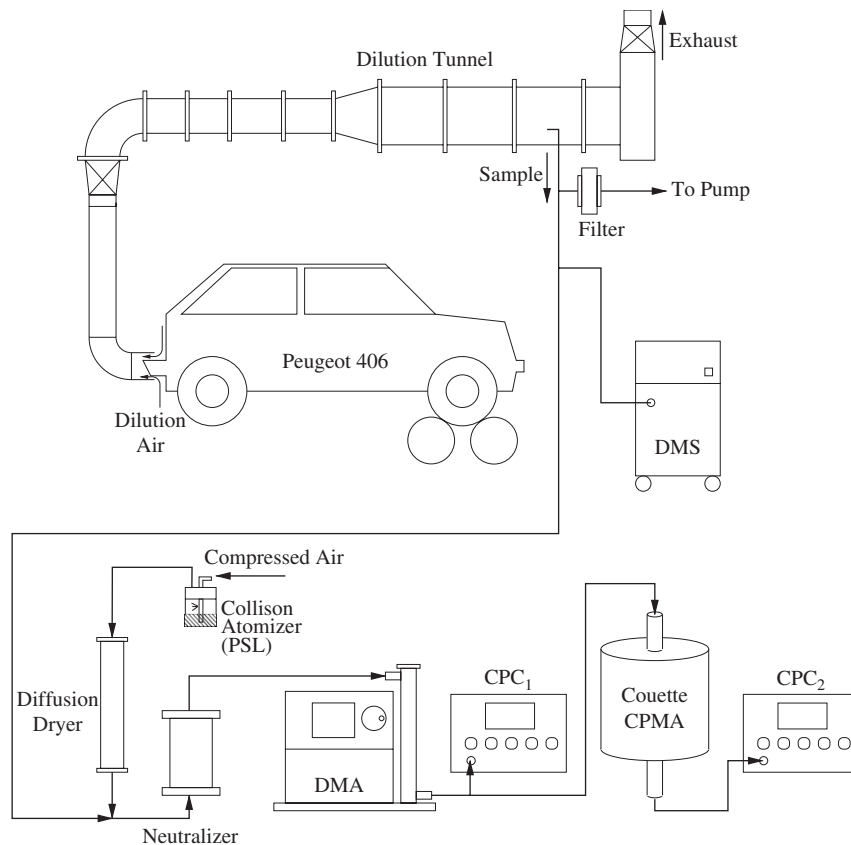
Fig. 1. Schematic of the experimental set-up.

(DMS500; Reavell et al., 2002) sampling from the dilution tunnel. Thirdly, the particle mass, effective density, and fractal dimension was measured with the DMA-Couette CPMA system described below.

2.2. The Couette CPMA

The Couette CPMA (see Olfert and Collings, 2005; Olfert et al., 2006) consists of two rotating coaxial cylindrical electrodes where the inner electrode is rotating slightly faster than the outer electrode. Charged particles that pass between the electrodes experience electrostatic and centrifugal forces acting in opposite directions. Depending on the rotational speed and voltage difference between the electrodes, particles of a particular mass-to-charge ratio will penetrate the Couette CPMA. The APM (Ehara et al., 1996) operates in a similar manner as the Couette CPMA, except that both electrodes rotate at the same angular velocity. In the APM some of the particles to be classified are lost due to an 'unstable' system of forces, which results in a decrease in the amplitude of the transfer function. The external forces acting on a charged particle in the APM are the centrifugal force which is proportional to r and the electrostatic force which is proportional to $1/r$ (where r is the distance from the axis of rotation to the particle). For a particle of the correct mass-to-charge ratio, these forces will be balanced at the so-called 'equilibrium radius', r^*. However, if the particle enters the gap between the electrodes at $r > r^*$, then the centrifugal force will be greater than the electrostatic force and the particle will diverge from the equilibrium radius and move toward the outer electrode (and vise versa for a particle entering the gap at $r < r^*$), where (depending on the operating conditions) it may impact on the electrode before exiting the classifier. Therefore, the system of external forces is unstable and the amplitude of the transfer function is decreased. The advantage of the Couette CPMA, compared to the APM, is that by rotating the inner electrode faster than the outer electrode, the centrifugal force will *decrease* as r increases so particles that enter the gap at $r > r^*$ or $r < r^*$ will converge toward the equilibrium radius and all of the particles of the correct mass-to-charge ratio will exit

the classifier. Therefore, the amplitude of the transfer function of the Couette CPMA will always be greater than or equal to the transfer function of the APM (Olfert and Collings, 2005).[1]

2.3. The DMA–CPMA system

Particles that were sampled by the DMA–CPMA system were passed through a radioactive charge neutralizer where they obtained a Boltzmann equilibrium charge distribution. The particles then enter the DMA (TSI model number 3080) where they were classified by mobility diameter. The DMA was set to an aerosol flow rate of 1.8 L/min and a sheath flow rate of 8 L/min. Condensation particle counters (CPCs) were used to measure the particle concentration before and after the Couette CPMA (CPC$_1$, TSI model number 3022A; CPC$_2$, TSI model number 3025A). The aerosol not counted by CPC$_1$ entered the Couette CPMA where the particles were classified by mass. The particles exiting the Couette CPMA were counted with CPC$_2$. The Couette CPMA was set at a constant rotational speed for each mobility size and the voltage was stepped. For a monodisperse aerosol (like that exiting the DMA) the transfer function of the Couette CPMA will be maximum when the centrifugal and electrostatic forces are balanced at the centre of the gap between the electrodes. At this point the mass of particles (m_c) exiting the Couette CPMA will be

$$m_c = \frac{neV_c}{\omega_c^2 r_c^2 \ln(r_2/r_1)},$$ (1)

where n is the number of elementary charges on the particle, e is the electronic charge, V_c is the voltage at which the transfer function is maximum, r_1 and r_2 are the inner and outer radii of the electrodes, r_c is the distance to the centre of the gap between the electrodes (i.e. $r_c = (r_1 + r_2)/2$), and ω_c is the angular velocity at r_c.

2.4. Measuring effective density

McMurry et al. (2002) showed that the effective density of particles can be accurately measured with a DMA–APM system by calibrating the system with polystyrene latex (PSL) particles. The same method can be used for the DMA–CPMA system used here. This is done by classifying PSL and diesel particles with the DMA–CPMA system, where the effective density of the diesel particle ($\rho_{\text{eff,diesel}}$) is

$$\rho_{\text{eff,diesel}} = \rho_{\text{p,diesel}} \frac{d_{\text{ve,diesel}}^3}{d_{\text{mo,diesel}}^3} = \rho_{\text{PSL}} \frac{V_{\text{c,diesel}}}{V_{\text{c,PSL}}},$$ (2)

where $\rho_{\text{p,diesel}}$ is the true density of the diesel particle, $d_{\text{ve,diesel}}$ and $d_{\text{mo,diesel}}$ are volume equivalent and mobility equivalent diameters of the diesel particle, ρ_{PSL} is the density of PSL (1.05 g/cm^3), and $V_{\text{c,diesel}}$ and $V_{\text{c,PSL}}$ are the voltages at which the transfer function is maximum for the diesel and PSL particles. As shown in previous work (Olfert et al., 2006), the maximum voltage can be found for each transfer function (i.e. $V_{\text{c,diesel}}$ and $V_{\text{c,PSL}}$) by fitting the data with a normal distribution function. The transfer function of the Couette CPMA (Ω) is defined as the ratio of the number concentrations of the aerosol exiting and entering the Couette CPMA,

$$\Omega = \frac{N_{\text{CPC}_2}}{N_{\text{CPC}_1}},$$ (3)

where N_{CPC_1} and N_{CPC_2} are the number concentrations from CPC$_1$ and CPC$_2$, respectively (see Fig. 1).

The accuracy of this system can be compromised by particles with multiple charges. The DMA will transmit multiply charged particles of the same electrical mobility but with a higher mass than the singly charged particles. Depending on the operating conditions of the Couette CPMA, some multiply charged particles may pass through the Couette CPMA

----

[1] Two new methods of improving the transfer function of the APM have been examined: the Couette CPMA and the Fluted CPMA. The Fluted CPMA has been described by Olfert (2005).
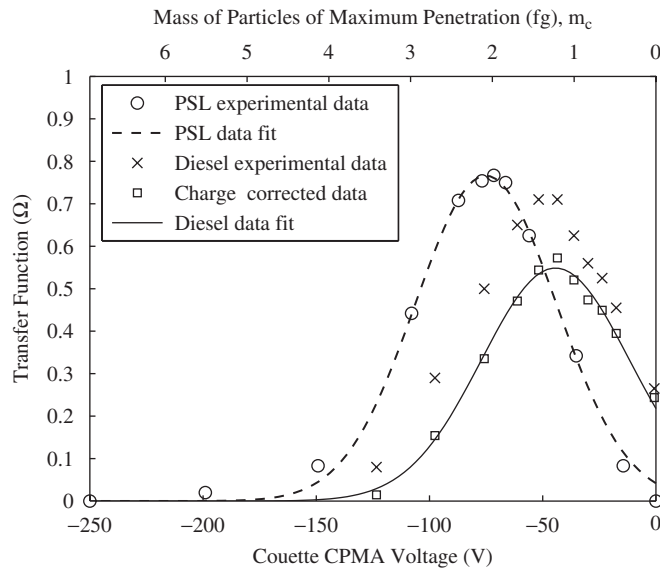
Mass of Particles of Maximum Penetration (fg), m_c

Fig. 2. The transfer function of the DMA–CPMA system classifying 152 nm PSL and diesel particles. The bottom x-axis shows the voltage steps of the Couette CPMA. For reference the top x-axis shows the mass of the particles of maximum penetration for the corresponding voltage step as determined by Eq. (1).

which will result in a higher effective density than expected. The data can be accurately corrected for multiple charging by employing the following method on the experimental data:

(1) Calculate the theoretical transfer function of the DMA in terms of electrical mobility using the experimental operating conditions of the DMA.
(2) Convert the transfer function of the DMA to mobility equivalent diameter for the number of charges that are to be considered and scale the transfer functions by the relative fraction of particles with the particular number of charges. In this study, up to three particle charges were considered and the charge distribution was calculated from the formulas given by Wiedensohler (1988) and Kim et al. (2005).
(3) Using the size distribution measured by the DMS, scale the transfer functions by the relative number of particles of each size.
(4) Assume a particle effective density function and converted the transfer functions into terms of specific mass (i.e. $m/(ne)$). A good first approximation of the effective density can be found by fitting the raw data at each mobility selected particle size with a normal distribution function to find $V_{c,diesel}$ and using Eq. (2) to find the effective density at each mobility size. The effective density function can then be found by fitting the effective density data with a power-law curve.
(5) Calculate the theoretical transfer function of the Couette CPMA (which is calculated in terms of specific mass) for each CPMA operating condition (i.e. for each voltage step of the CPMA) and multiply the transfer functions of the DMA and Couette CPMA together.
(6) Calculate the fraction of singly charged particles to the total number of particles that where transmitted through the DMA–CPMA system for each voltage step.
(7) Scale the experimental transfer function of the combined DMA–CPMA system by the fraction of singly charged particles and recalculate the effective density.
(8) Compare the new effective density to the previous effective density and repeat steps (4)–(7) until a desired tolerance is reached. In this study a tolerance of 1% was used.

An example of measuring the effective density of diesel particles using the method described above is seen in Fig. 2. The figure shows the penetration of 152 nm PSL and diesel particles through the DMA–CPMA system. The penetration of diesel particles is also shown when the correction is applied for multiple charging. The effective density is calculated

by fitting the PSL and diesel data with normal distribution functions to find the CPMA voltage of maximum penetration and applying Eq. (2). Using this method the effective density of the 152 nm diesel particles in this test was $0.620\,g/cm^3$. Previously, it was shown that this DMA–CPMA system could measure the density of spherical oil particles to within approximately 3% of the actual density (Olfert et al., 2006). Since the same experimental set-up and conditions were used in this study, we will assume the uncertainty in the effective density measurement in this study to be 3%.

2.5. Measuring fractal dimension

Schmidt-Ott et al. (1990) have shown that a power-law relationship can be used to correlate particle mass and mobility experimental data to find the fractal dimension (D_f) of agglomerate particles. Skillas et al. (1998) showed that the mass of a particle is related to its mobility diameter and fractal dimension by the following relationship:

$$m \propto d_{mo}^{D_f}. \tag{4}$$

When using a DMA–CPMA system calibrated with PSL, the mass of a test particle will be

$$m_{diesel} = \rho_{PSL} \frac{\pi d_{mo}^3}{6} \frac{V_{c,diesel}}{V_{c,PSL}}. \tag{5}$$

The fractal dimension of the diesel particles was found by plotting the mass of the particles by their mobility diameter and fitting the data using a least-squares fit with a power-law relationship. In the fitting procedure, the relative error between the fit and the experimental data was used so that each data point was properly weighted. The uncertainty in the fractal dimension measurement can be estimated by the numerical 'jackknife' method. The uncertainty of the fractal dimension reported in this work is stated with 95% confidence.

3. Experimental results and discussion

3.1. The effect of DOCs and fuel sulphur content

The vehicle was tested at six different steady-state operating conditions ranging in engine load and engine speed, as shown in Table 1. For each of the operating conditions the size distribution of the exhaust was continually measured with the DMS and the average size distribution over a particular time is shown in Fig. 3 (the durations shown correspond to the times of the first or second filter sampling). The figure shows the differences in the size distributions of the operating conditions. Note that in Figs. 3a–d (lower loads) the size distributions have a single accumulation mode; while in Figs. 3e–f (higher loads) the distributions have a nucleation and accumulation mode. Filter papers from tests 3 to 6 were analysed for sulphates and these results are summarized in Table 2. The sulphate analysis shows that at 15% engine load the combined mass of sulphate and water was 1.8–2.3% of the total particulate mass. This was much lower than the mass fraction of sulphate/water at higher engine loads where the mass fraction ranged from 17.4% at 35% load to 29.0% at 40% load. Therefore, we assume that the nucleation mode seen at high engine loads is due to increased levels of sulphuric acid in the exhaust which is known to trigger nucleation.

Several studies have shown that vehicles with a DOC and high-sulphur fuel will produce a nuclei mode at high engine load (Maricq et al., 2002; Vogt et al., 2003; Giechaskiel et al., 2005). Vogt et al. (2003) and Giechaskiel et al. (2005)

Table 1
Summary of test conditions and fractal dimension measurements

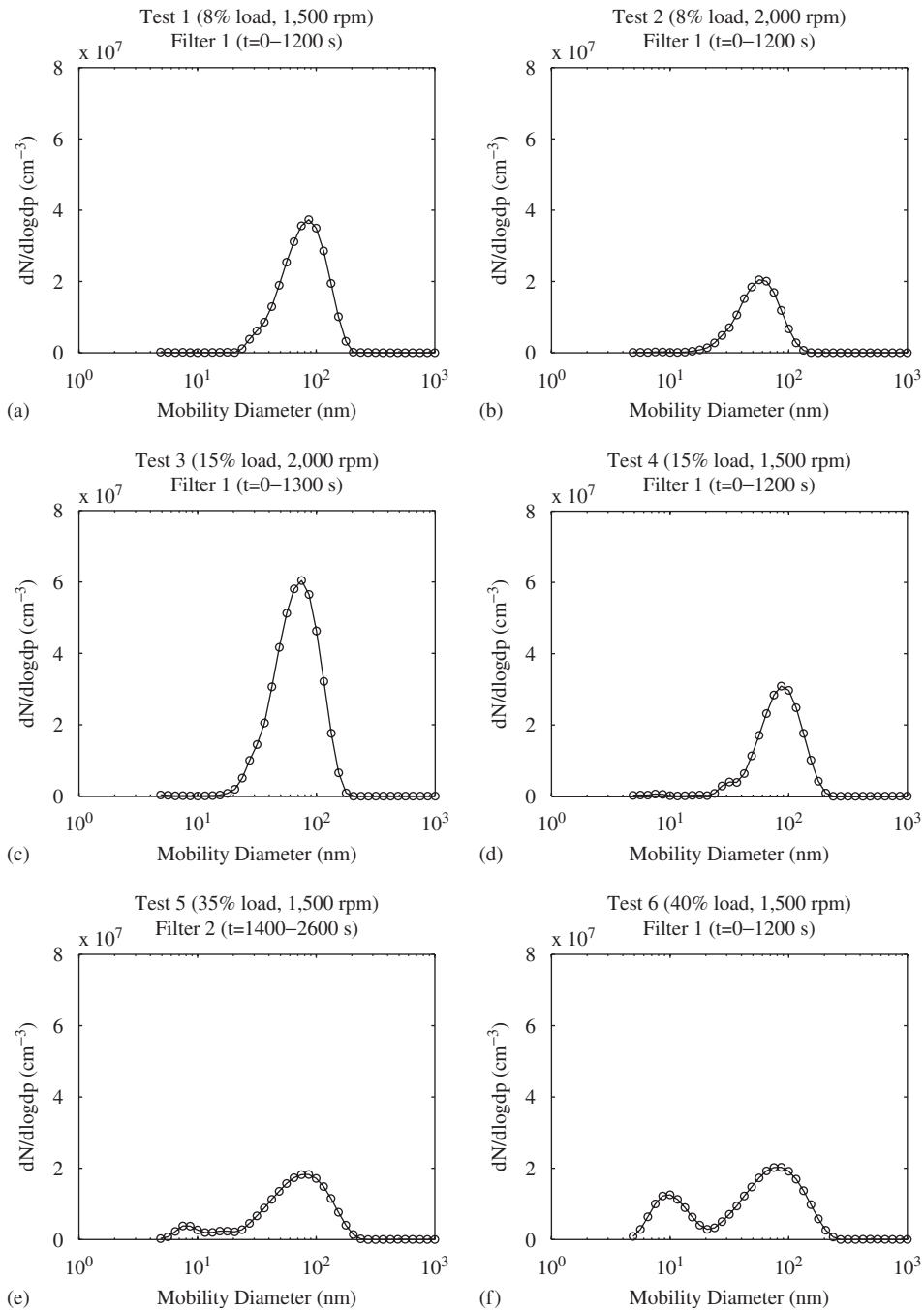| Test	Engine load (%)	Engine speed (rpm)	Dilution ratio	Average DOC temperature (°C)	Fractal dimension
1	8	1500	6.2:1	197	2.48 ± 0.10
2	8	2000	4.0:1	204	2.34 ± 0.20
3	15	2000	3.9:1	250	2.22 ± 0.30
4	15	1500	5.8:1	240	2.36 ± 0.16
5	35	1500	2.8:1	310	2.47 ± 0.24
6	40	1500	2.7:1	336	2.76 ± 0.06

Fig. 3. The time-averaged size distributions from a light-duty diesel engine as measured with a DMS500. The time intervals correspond to the time of filter sampling.

conducted real-world chase experiments where they sampled a light-duty diesel vehicle's exhaust in the atmosphere. Both of these studies found that a nucleation mode was only present at high engine loads (at vehicle speeds of approximately 100–120 km/h) when the DOC was present. When the DOC was removed no nucleation mode was detected. Vogt et al. (2003) also showed that when low-sulphur fuel (40 ppm) was used no nucleation mode was present. Giechaskiel et al. (2005) repeated the tests in the laboratory, sampling from a system with much lower dilution ratios

Table 2
Sulphate analysis of filter papers

Test	Total mass of particulates (mg)	Mass of sulphates (mg)	Mass of water[a] (mg)	Mass fraction of sulphates and water (%)
Test 3 (15% load)—Filter 1	0.795	0.0079	0.0103	2.3
Test 4 (15% load)—Filter 1	0.740	0.0057	0.0074	1.8
Test 5 (35% load)—Filter 2	0.621	0.0470	0.0611	17.4
Test 6 (40% load)—Filter 1	0.951	0.1200	0.1560	29.0

[a]The mass of water that is chemically combined with sulphuric acid is approximately 1.3 times the measured sulphate.

($\sim 13:1$) than atmospheric dilution, and found that the nucleation mode was present at the same operating conditions. Giechaskiel et al. (2005) conclude that the nucleation mode is not a dilution or sampling artefact but rather a true vehicle emission. Maricq et al. (2002) conducted similar experiments in a wind tunnel, sampling from the wind tunnel and directly from the tail pipe. They found that a nucleation mode was only present at high engine loads when a high-sulphur fuel (350 ppm) and an active DOC were used (using low-sulphur fuel (4 ppm), or high-sulphur fuel without a DOC, no nucleation mode was measured). All of the authors (Maricq et al., 2002; Vogt et al., 2003; Giechaskiel et al., 2005) suppose that at higher DOC temperatures (when operating at high engines loads) the DOC converts more SO_2 to SO_3. As the exhaust cools the SO_3 nucleates to hydrated H_2SO_4 particles. Giechaskiel et al. (2005) also suggest that the increased fuel consumption at higher loads would increase the concentration of SO_2 available for the formation of sulphuric acid. All of the authors also noticed a time-dependence of the nucleation mode at some operating conditions. These authors suppose that sulphur may be stored in the DOC and exhaust system at low exhaust temperatures and is released when the storage limit is reached.

The results shown in this work seem to support these previous studies. At high loads (Figs. 3e–f) a nucleation mode was present while at low loads no nucleation mode was present (Figs. 3a–d). Table 1 shows the average temperature of the DOC during each test. At high loads the temperature of the DOC is higher (310–336 °C) than at lower loads (197–250 °C), which supports the theory that more SO_2 is converted to SO_3 at higher temperatures in a DOC. This is further verified by the sulphate analysis of the filter samples, where at higher loads and hotter DOC temperatures the mass fraction of sulphate/water was more than an order of magnitude higher than at lower loads and DOC temperatures.

One difference between the results shown here and that of the Vogt et al. (2003) study is that Vogt et al. (2003) did not measure a nucleation mode when fuel with 40 ppm of sulphur was used at high load; however, a nucleation mode was measured in this study at high load when fuel with ~ 50 ppm of sulphur was used. This difference is most likely due to the difference in DOC temperatures. In the Vogt et al. (2003) high load test the DOC temperature was 270 °C, while the DOC temperatures at high load in this study were 310–336 °C. Therefore, we assume that the higher DOC temperatures in this study were sufficient to produce enough sulphuric acid for nucleation.

It is important to note that the type of sampling system used in sampling the engine exhaust can have a large effect on the particle properties. In different sampling systems the properties of particles can change due to coagulation, nucleation, adsorption/desorption, and condensation/evaporation and the effect of these processes will be related to the dilution ratio, residence time and the dilution air's temperature and humidity (Kittelson et al., 1999). In Table 1 the dilution ratios for the tests are listed. The dilution ratios in the CVS tunnel used in this test are generally lower than other sampling systems (i.e. atmospheric sampling). At lower dilution ratios the saturation ratio of sulphuric acid will be higher, which leads to a higher probability of the nucleation of sulphuric acid. Therefore the effects of sulphate condensation on the particle properties in these tests maybe greater than at higher dilution ratios. Also, as shown in Table 1 at higher engine loads, when nucleation modes were present, the dilution ratios were 2.7–2.8:1, while at lower engine loads the dilution ratios ranged from 3.9 to 6.2:1, which results in higher saturation ratios at lower dilution ratios. Therefore, the nucleation mode particles witnessed at higher engine loads may have been formed due to the increase in SO_3 concentration at higher DOC temperatures and higher saturation ratios of sulphuric acid at lower dilution ratios.

3.2. Effective density

For each of the operating conditions the effective density of the particles was measured over a range of mobility sizes, typically between 50 and 299 nm. The effective densities of the diesel particles are shown in Fig. 4. In all of the
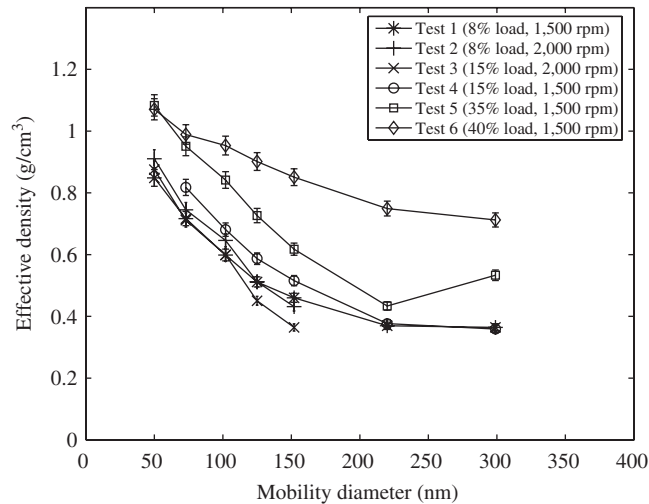
Fig. 4. Comparison of the effective densities of diesel particles from a light-duty diesel vehicle at various engine operating conditions.

tests the effective density decreased with an increase in particle size, as would be expected with agglomerated particles. In diesel soot, primary particles (typically between 20 and 50 nm in size, Witze, 2001) agglomerate into chain-like structures. It follows that smaller particles (i.e. 50 nm) will be more compact than larger particles, and therefore will have a higher effective density.

The figure also shows that the effective densities of the aerosol with no nucleation mode, and lower sulphate levels (i.e. tests 1–4) are very similar. However, at higher loads, when sulphate levels were considerably higher, the effective density of the particles increased dramatically. From this data it seems that when there are higher levels of sulphate, sulphuric acid is condensing onto the soot agglomerate particles and increasing their effective density. The exact mechanism that condensed sulphuric acid has on increasing the effective density of a particle is unclear. Sulphuric acid is inherently denser than other condensed material ($\sim 1.84\,\text{g/cm}^3$ (at 95% conc.) compared to $\sim 0.9\,\text{g/cm}^3$ for hydrocarbons, and $1\,\text{g/cm}^3$ for water) so the addition of condensed sulphuric acid may increase the density of a particle. However, sulphuric acid may increase the adsorption of hydrocarbons and sulphuric acid is highly hygroscopic, both of which will decrease the density of the condensed matter (Kittelson, 2006). The sulphuric acid will fill internal and external voids in the particle. The condensed material would increase the mass of the particle but this would have a relatively small effect on the drag (and thus the measured mobility diameter) of the particle; therefore the effective density of the particle will increase. The increase in effective density from 35% to 40% load is presumably due to the fact that at higher DOC temperatures more SO_3 is available for sulphuric acid formation, as seen in the filter paper analysis, which leads to more sulphuric acid condensing on the soot agglomerate. A similar result was found by Park, Cao et al. (2003) who measured the effective density of particles from a light-duty diesel engine with high-sulphur (360 ppm) and low-sulphur fuel (~ 0 ppm). They found that the effective density of an 83 nm particle increased from 0.90 to $1.10\,\text{g/cm}^3$ when high-sulphur fuel was used. The study did not mention if the vehicle was fitted with a DOC.

The effective density results from this study have been compared to other studies in Fig. 5. In the studies by Park, Cao et al. (2003) and Park et al. (2003), a heavy-duty diesel engine was tested at 10%, 50%, and 75% load. At low load (10%), a large nucleation mode was present, which was assumed to be mostly comprised of hydrocarbons, while at higher engine loads (50% and 75%), no nucleation mode was present. The results from Park, Cao et al. (2003) study (shown in Fig. 5) show that when the nucleation mode was present the effective density of the particles did increase, especially at smaller particles sizes. In this current study, we presume that the majority of the condensible material was sulphuric acid rather than volatile hydrocarbons. The experimental results seem to suggest that condensed sulphate material on accumulation mode particles increases the effective density of the particles by a greater degree than hydrocarbon material.

Fig. 5 also shows that the effective density of particles in this study when no nucleation mode was present and sulphate levels were lower (test 1) is similar to the measurements made by Park, Cao et al. (2003) (at 75% engine
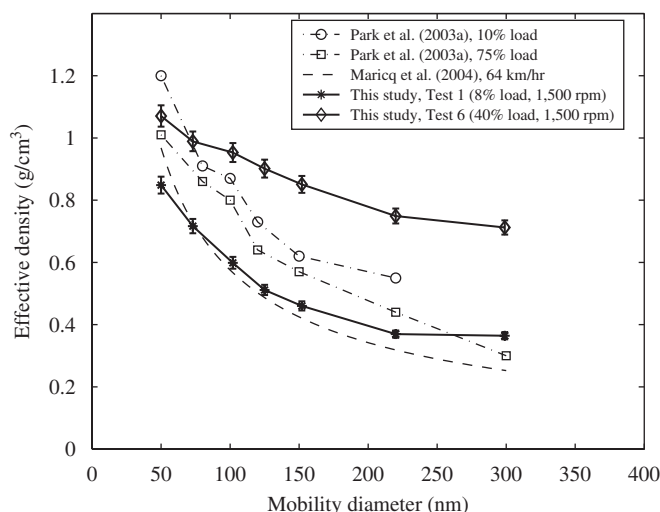
Fig. 5. The effective densities of diesel particles from this and other studies.

load when no nucleation mode was present) and Maricq and Xu (2004). It should be noted that Maricq and Xu (2004) used a CVS dilution tunnel, similar to the one used in this study, and a constant-volume rapid exhaust dilution system. Maricq and Xu (2004) found that both dilution systems produced very similar results (at 64 km/h the results were 'indistinguishable' and at 112 km/h the effective densities from the rapid exhaust dilution system were about 10% higher). In our study, an advanced dilution system was not available, but our results, when sulphate levels were lower, are similar to Park, Cao et al. (2003) (at 75% load) and Maricq and Xu (2004) considering the differences in engine and after-treatment technologies.

Previously, Vaaraslahti et al. (2005) have shown that considerable amounts of sulphur can be stored in after-treatment devices and this sulphur can be released at higher exhaust temperatures. Therefore, even in the steady-state tests performed here, the amount of released sulphate may change during the test which may change the size distribution, as evidenced by a change in the nucleation mode. In this study a time-dependence of the nucleation mode was seen at high engine loads. Fig. 6 shows the evolution of the size distributions of tests 5 and 6 over time. In test 5 (Fig. 6a) initially there was a small accumulation mode and near the midpoint of the test the nucleation mode began to grow until it reached its maximum value at the end of the test. The nucleation mode may have grown over time due to an increased rate of stored sulphur release as the DOC temperature increased or perhaps more SO_2 was converted to SO_3 near the end of the test due to an increase in DOC temperature (the DOC temperature was approximately 13 °C higher at the end of the test). In test 6 (Fig. 6b), a large nucleation mode was present near the start of the test which decayed over time. In this test the DOC was approximately 26 °C higher than test 5, so perhaps any stored sulphur was released near the start of the test until most of the stored sulphur was released. A limitation of the DMA–CPMA system is that it takes on the order of 10 min to measure the density of one mobility-selected size class and approximately 1 h to measure the entire range of particle sizes (each density measurement was made in no particular order during each test). Therefore, the effective densities of particles may change during the test. This may account for the relatively high effective density measurement at 299 nm on test 5, since it was the last measurement in that test when the nucleation mode was the largest, and presumably when higher amounts of sulphur where emitted. Although there was a nucleation mode present for the duration of both tests 5 and 6, it is not clear if the change in magnitude of the nucleation mode (presumably from changes in exhaust sulphur levels) resulted in changes in the effective densities of particles in the accumulation mode.

3.3. Fractal dimension

The mass-mobility relationship for each of the tests is shown in Fig. 7. The fractal dimension for the particles in each of the tests is found by fitting the mass-mobility data with a power-law function. The fractal dimension measured for
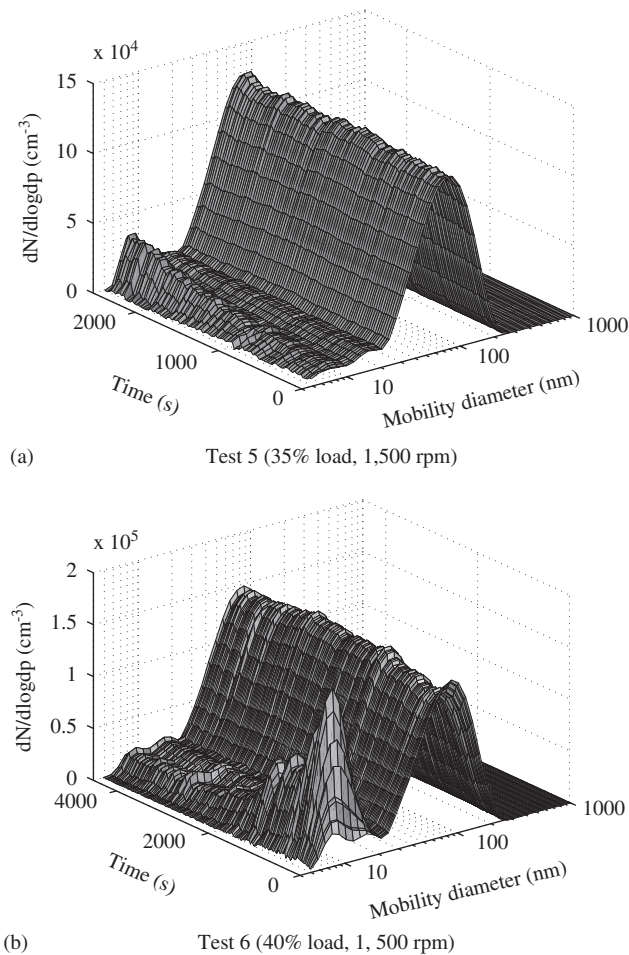
Fig. 6. Time-dependent size distributions of the exhaust of the light-duty diesel engine in test 5 and 6: (a) test 5 (35% load, 1500 rpm); (b) test 6 (40% load, 1500 rpm).

each of the tests are found in Table 1. At lower engine loads, when sulphate levels were lower and no nucleation mode was present, the fractal dimension ranged between 2.22 and 2.48. When sulphate levels were higher at higher engine loads, the fractal dimension was measured to be much higher (2.47–2.76).

A summary of various studies on the fractal dimension of diesel particles are shown in Table 3. The experimental results and the interpretation of the experimental results of the fractal dimension of diesel particles differ in the literature. Park, Cao et al. (2003), Skillas et al. (1998), and Virtanen, Ristimäki, Vaaraslahti et al. (2004) all suggest that the fractal dimension of diesel particles decrease with an increase in engine load. Park, Cao et al. (2003) found that the fractal dimension of diesel particles from a heavy-duty engine decreases from 2.41 at 10% load to 2.33 at 75%. Park, Cao et al. (2003) suggest that for heavy-duty engines at lower engine loads more volatile material is available in the exhaust and it condenses on the particles which fills in the voids of the particle, thereby making the particle more compact which increases the fractal dimension. Skillas et al. (1998) measured the fractal dimension of particles from a diesel generator and found the fractal dimension varied from approximately 2.3 to 2.9, with the fractal dimension generally decreasing with an increase in engine load. Skillas et al. (1998) suggest that at low engine loads ballistic particle–cluster agglomeration dominates which results in a high fractal dimension ($\sim$ 3 according to theory; Friedlander, 2000) and at high engine loads cluster–cluster agglomeration dominates, which leads to much lower fractal dimensions ($\sim$ 2 according to theory). Virtanen, Ristimäki, Vaaraslahti et al. (2004) tested a light-duty and heavy-duty diesel engine and found that the fractal dimension for both vehicles decreased from 2.8 at low loads to 2.6 at high loads. In general, the fractal dimensions measured by Virtanen, Ristimäki, Vaaraslahti et al. (2004) are higher than other studies.
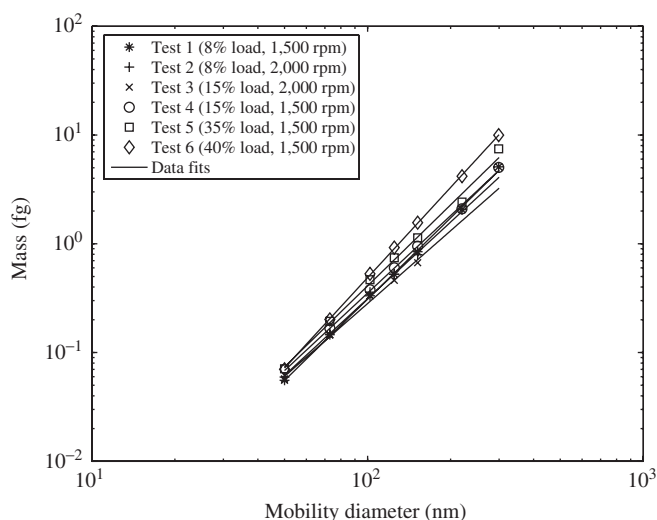
Fig. 7. The size-dependent mass of particles from a light-duty diesel vehicle.

Table 3
Summary of fractal dimension measurements for diesel particulates

Study	Engine description	Technique	Load or veh. speed	Fractal dimension
Park, Cao et al. (2003)	John Deere 4045 (4.5 L/75 kW)	DMA-APM	10% 75%	2.41 ± 0.02 2.33 ± 0.03
Maricq and Xu (2004)	TDI[a] (1.9 L) & TDI (1.8 L)	DMA-ELPI	64 km/h 113 km/h	2.25 ± 0.1 2.20 ± 0.1
Skillas et al. (1998)	Yamaha EDA3000 (3.3 kW generator)	DMA-ELPI	0% 15% 45% 60% 76%	~ 2.9 ~ 2.9 ~ 2.4 ~ 2.3 ~ 2.6
Virtanen, Ristimäki, Vaaraslahti et al. (2004)	TDI (1.9 L/66 kW) & TDI (9.6 L/210 kW)	SMPS-ELPI	'Low load' 'High load'	~ 2.8 ~ 2.6
Van Gulijk et al. (2004)	Lister-Petter generator (0.9 L/ 5.7 kW)	DMA-ELPI	50%	2.42 ± 0.12

[a]Turbo Direct Injection.

As mentioned above, Virtanen, Ristimäki, Vaaraslahti et al. (2004) uses a parallel SMPS–ELPI fitting method to calculate the fractal dimension. The advantage of the parallel method is that only a single measurement is needed to calculate the fractal dimension while a series method, like the DMA–ELPI method (used by Skillas et al., 1998; Maricq and Xu, 2004) or DMA–CPMA method, requires time consuming point by point measurements over the range of mobility sizes. However, the disadvantage of the parallel SMPS–ELPI method is that the measurement is weighted by the number concentration of the particles. The peak of diesel soot size distributions typically range from 50 to 80 nm, so the fractal dimension measurement with this system will be biased to the fractal dimension of the particles in that size range. This size peak is typically in a transition regime between the size of primary particles (20–50 nm) that will have a fractal dimension of 3 and the truly aggregate particles at larger particle sizes which typically have a fractal dimension of ~ 2.2–2.5. Therefore, for typical diesel soot size distributions, the parallel SMPS–ELPI method will measure a higher fractal dimension than what would be expected. Virtanen, Ristimäki, Vaaraslahti et al. (2004) verified this by measuring the fractal dimension of particles with the parallel SMPS–ELPI method and with the series DMA–ELPI method. For that test the SMPS–ELPI method produced a result of 2.6, while the DMA–ELPI gave a fractal dimension of 2.6 for the range of particles sizes of ~ 50–80 nm (where the number concentration was highest), and a fractal dimension of

2.3 for particle sizes between ~ 80 and 200 nm. Therefore, the difference in fractal dimension used in the Virtanen, Ristimäki, Vaaraslahti et al. (2004) study compared to other studies is most likely due to measurement method alone.

While the above studies state that there is a dependence between fractal dimension and engine load, Maricq and Xu (2004) state that the fractal dimension is relatively independent of speed, load, or driving mode. Maricq and Xu (2004) measured the fractal dimension of soot from a premixed ethylene flame (2.15 ± 0.1), a light-duty diesel engine (2.3 ± 0.1), and a direct injection spark ignition vehicle (2.3 ± 0.1). Maricq and Xu (2004) also noted that the effective density of particles is almost constant below ~ 50 nm.

The fractal dimensions measured in this study at lower loads and sulphate levels agree well with Park, Cao et al. (2003), Maricq and Xu (2004), and Van Gulijk et al. (2004). In all of these studies (which included diesel generators and light and heavy-duty diesel vehicles) the fractal dimension is surprisingly similar, being in the range of 2.2–2.48. Some of the studies noticed a increase in fractal dimension with an decrease in engine load due to an increase in volatile hydrocarbons at lower loads. The opposite was measured here because at high engine loads sulphate levels increased, which resulted in increased amounts of sulphuric acid condensing on the soot agglomerates. This has the effect of significantly increasing the fractal dimension of the particles. Although, with so much liquid material condensed on the particles (recall that 29% of the total particulate mass in test 6 was sulphates and water), the particles may not be considered truly fractal. Nevertheless, the fractal dimension is a useful concept for comparing particle properties because even with cases of high condensation the fractal dimension gives an indication of the amount of condensation that has taken place.

4. Summary

The effective density and fractal dimension of particles from a light-duty diesel vehicle was measured with a DMA and a Couette CPMA. The vehicle was fitted with a diesel oxidation catalyst (DOC) and it was found that at high loads the DOC would increase in temperature, sulphate levels would increase and a nucleation mode was formed. Filter paper sulphate analysis showed that at higher engine loads and hotter DOC temperatures, sulphate levels increased. Previous studies have shown that high sulphur fuel and a hot DOC can lead to the formation of a nucleation mode triggered by an increase in sulphate levels (Maricq et al., 2002; Vogt et al., 2003; Giechaskiel et al., 2005).

It was found that when sulphate levels were lower at low engine loads, the effective density of the particles ranged from ~ 0.9 g/cm^3 at 50 nm to ~ 0.4 g/cm^3 at 299 nm. At a relatively high engine load of 40% and high sulphate levels, the effective density of the particle increased dramatically to ~ 1.07 g/cm^3 at 50 nm to ~ 0.71 g/cm^3 at 299 nm. Park, Cao et al. (2003) noticed a similar increase in density when high-sulphur fuel was used.

At low engine loads and lower sulphate levels, the fractal dimension of the particles ranged from about 2.22 to 2.48. The fractal dimensions measured at low load agreed well with previous studies (i.e. 2.33–2.41, Park, Cao et al., 2003; 2.3 ± 0.1 Maricq and Xu, 2004; 2.4, Van Gulijk et al., 2004). Some authors have found that the fractal dimension increases with a decrease in engine load (Park, Cao et al., 2003, Virtanen, Ristimäki, Vaaraslahti et al., 2004); however, the same result was not found here because at high engine loads the sulphate levels increased which resulted in increased amounts of sulphuric acid condensing on the soot agglomerates, which resulted in fractal dimensions as high as 2.76 at 40% load.

References

Ahlvik, P., Ntziachristos, P., Keskinen, J., & Virtanen, A. (1998). Real time measurements of diesel particle size distribution with an electrical low pressure impactor. Society of Automotive Engineers, 980410.

Bérubé, K. A., Jones, T. P., Williamson, B. J., Winters, C., Morgan, A. J., & Richards, R. J. (1999). Physicochemical characterisation of diesel exhaust particles: Factors for assessing biological activity. *Atmospheric Environment*, 33, 1599–1614.

Ehara, K., Hagwood, C., & Coakley, K. J. (1996). Novel method to classify aerosol particles according to their mass-to-charge ratio—aerosol particle mass analyser. *Journal of Aerosol Science*, 27, 217–234.

Friedlander, S. K. (2000). *Smoke, dust, and haze: Fundamentals of aerosol dynamics*. Oxford: Oxford University Press.

Giechaskiel, B., Ntziachristos, L., Samaras, Z., Scheer, V., Casati, R., & Vogt, R. (2005). Formation potential of vehicle exhaust nucleation mode particles on-road and in the laboratory. *Atmospheric Environment*, 39, 3191–3198.

Hand, J. L., & Kreidenweis, S. M. (2002). A new method for retrieving particle refractive index and effective density from aerosol size distribution data. *Aerosol Science and Technology*, 36, 1012–1026.

Katrib, Y., Martin, S. T., Rudich, Y., Davidovits, P., Jayne, J. T., & Worsnop, D. R. (2004). Density changes of aerosol particles as a result of chemical reaction. *Atmospheric Chemistry and Physics Discussions*, 4, 6431–6472.

Kim, J. H., Mulholland, G. W., Kukuck, S. R., & Pui, D. Y. H. (2005). Slip correction measurements of certified PSL nanoparticles using a nanometer differential mobility analyzer (Nano-DMA) for Knudsen number from 0.5 to 83. *Journal of Research of the National Institute of Standards and Technology*, *110*, 31–54.

Kittelson, D. (2006). Personal communication.

Kittelson, D., Arnold, M., & Watts, W. F., Jr. (1999). *Review of diesel particulate matter sampling methods*. Technical Report, Environmental Protection Agency.

Maricq, M. M., Chase, R. E., Xu, N., & Laing, P. M. (2002). The effects of the catalytic converter and fuel sulfur level on motor vehicle particulate matter emissions: Light duty diesel vehicles. *Environmental Science and Technology*, *36*, 283–289.

Maricq, M. M., Podsiadlik, D. H., & Chase, R. E. (2000). Size distributions of motor vehicle exhaust PM: A comparison between ELPI and SMPS Measurements. *Aerosol Science and Technology*, *33*, 239–260.

Maricq, M. M., & Xu, N. (2004). The effective density and fractal dimension of soot particles from premixed flames and motor vehicle exhaust. *Journal of Aerosol Science*, *35*, 1251–1274.

McMurry, P. H., Wang, X., Park, K., & Ehara, K. (2002). The relationship between mass and mobility for atmospheric particles: A new technique for measuring particle density. *Aerosol Science and Technology*, *36*, 227–238.

Olfert, J. S. (2005). A numerical calculation of the transfer function of the fluted centrifugal particle mass analyzer. *Aerosol Science and Technology*, *39*, 1002–1009.

Olfert, J. S., & Collings, N. (2005). New method for particle mass classification—The Couette centrifugal particle mass analyzer. *Journal of Aerosol Science*, *36*, 1338–1352.

Olfert, J. S., Reavell, K. StJ., Rushton, M. G., & Collings, N. (2006). The experimental transfer function of the Couette centrifugal particle mass analyzer. *Journal of Aerosol Science*, in press, doi:10.1016/j.jaerosci.2006.07.007.

Park, K., Cao, F., Kittelson, D. B., & McMurry, P. H. (2003). Relationship between particle mass and mobility for diesel exhaust particles. *Environmental Science and Technology*, *37*, 577–583.

Park, K., Kittelson, D. B., & McMurry, P. H. (2003). A closure study of aerosol mass concentration measurements: Comparison of values obtained with filters and by direct measurements of mass distributions. *Atmospheric Environment*, *37*, 1223–1230.

Reavell, K., Hands, T. & Collings, N. (2002). A fast response particulate spectrometer for combustion aerosols. Society of Automotive Engineers, 2002-01-2714.

Ristimäki, J., Virtanen, A., Marjamäki, M., Rostedt, A., & Keskinen, J. (2002). On-line measurement of size distribution and effective density of submicron aerosol particles. *Journal of Aerosol Science*, *33*, 1541–1557.

SAE J1936 (1989). Chemical methods for the measurement of nonregulated diesel emissions. Society of Automotive Engineers, Recommended Practice J1936.

Schmidt-Ott, A., Baltensperger, U., Gäggeler, H. G., & Jost, D. T. (1990). Scaling behaviour of physical parameters describing agglomerates. *Journal of Aerosol Science*, *21*, 711–717.

Skillas, G., Künzel, S., Burtscher, H., Baltensperger, U., & Siegman, K. (1998). High fractal-like dimension of diesel soot agglomerates. *Journal of Aerosol Science*, *29*, 411–419.

Vaaraslahti, K., Keskinen, J., Giechaskiel, B., Soola, A., Murtonen, T., & Vesala, H. (2005). Effect of lubricant on the formation of heavy-duty diesel exhaust nanoparticles. *Environmental Science and Technology*, *39*, 8497–8504.

Van Gulijk, C., Marijnissen, J. C. M., Makkee, M., Moulijn, J. A., & Schmidt-Ott, A. (2004). Measuring diesel soot with a scanning mobility particle sizer and an electrical low-pressure impactor: Performance assessment with a model for fractal-like agglomerates. *Journal of Aerosol Science*, *35*, 633–655.

Virtanen, A., Ristimäki, J., & Keskinen, J. (2004). Method for measuring effective density and fractal dimension of aerosol agglomerates. *Aerosol Science and Technology*, *38*, 437–446.

Virtanen, A., Ristimäki, J., Marjamäki, M., Vaaraslahti, K., Keskinen, J., & Lappi, M. (2002). Effective density of diesel exhaust particles as a function of size. *Society of Automotive Engineers*, 2002-01-0056.

Virtanen, A. K. K., Ristimäki, J. M., Vaaraslahti, K. M., & Keskinen, J. (2004). Effect of engine load on diesel soot particles. *Environmental Science and Technology*, *38*, 2551–2556.

Vogt, R., Scheer, V., Casati, R., & Benter, T. (2003). On-road measurement of particle emission in the exhaust plume of a diesel passenger car. *Environmental Science and Technology*, *37*, 4070–4076.

Wiedensohler, A. (1988). Technical note: An approximation of the bipolar charge distribution for particles in the submicron range. *Journal of Aerosol Science*, *19*, 387–389.

Witze, P. O. (2001). Diagnostics for the measurement of particulate matter emissions from reciprocating engines. *The fifth international symposium on diagnostics and modeling of combustion in internal combustion engines* (*COMODIA*), July 1–4, Nagoya.

Zelenyuk, A., Cai, Y., Chieffo, L., & Imre, D. (2005). High precision density measurements of single particles: The density of metastable phases. *Aerosol Science and Technology*, *39*, 972–986.